EDGE ARTICLE

CrossMark
← click for updates

Redox non-innocence permits catalytic nitrene carbonylation by (dadi)Ti═NAd (Ad = adamantyl)†

Spencer P. Heins,[a] Peter T. Wolczanski,[*a] Thomas R. Cundari[*b] and Samantha N. MacMillan[a]

Application of the diamide, diimine {−CH═N(1,2-C_6H_4)N(2,6-$^iPr_2$-C_6H_3)}$_2^m$ ((dadi)^m) ligand to titanium provided adducts (dadi)TiL$_x$ (**1**-L$_x$; L$_x$ = THF, PMe$_2$Ph, (CNMe)$_2$), which possess the redox formulation [(dadi)$^{4-}$]Ti(IV)L$_x$, and 22 πe$^-$ (4n + 2). Related complexes containing titanium-ligand multiple bonds, (dadi)Ti═X (**2**═X; X = O, NAd), exhibit a different dadi redox state, [(dadi)$^{2-}$]Ti(IV)X, consistent with 20 πe$^-$ (4n). The Redox Non-Innocence (RNI) displayed by dadi^m impedes binding by CO, and permits catalytic conversion of AdN$_3$ + CO to AdNCO + N$_2$. Kinetics measurements support carbonylation of **2**═NAd as the rate determining step. Structural and computational evidence for the observed RNI is provided.

Introduction

The diamide, diimine {−CH═N(1,2-C_6H_4)N(2,6-$^iPr_2$-C_6H_3)}$_2^m$ (m = 0 to −4), *i.e.* (dadi)^m, was previously introduced as a tetradentate chelate ligand capable of at least 5 redox states.[1] In the initial study, (dadi)M (M = Cr(THF), Fe) was shown to transfer azide-generated nitrenes into carbon–carbon bonds *via* aziridination. In the process the dadi^{2-} ligand (20 πe$^-$, 4n) was derivatized to a 22 πe$^-$ (4n + 2) ligand (*i.e.*, [RN{CH═N(1,2-C_6H_4)N(2,6-$^iPr_2$-C_6H_3)}$_2$]$^{2-}$M^{II} (R = 2,6-$^iPr_2C_6H_3$, adamantyl (Ad))) of considerable stability.

Redox non-innocent (RNI) ligands[1–20] like dadi^m can support catalytic activity[11–17] by expanding the redox capability of a system, essentially electronically buffering the transition metal center. As Fig. 1 illustrates, a ligand capable of RNI can keep the metal in a stable configuration (M^{m+2}) by being in a reduced state (L^p → L^{p-2}), and releasing the electrons to the metal upon oxidative addition of XY (L^{p-2}M^{m+2} → L^{p}M^m → L^{p}M^{m+2}XY). Transfer of XY to a substrate, perhaps *via* a binding step, causes reduction of the metal, but its formal oxidation state is maintained (M^m → M^{m+2}) by the RNI of the ligand.

In its dianionic (n = −2) state, (dadi)^m possessed a 4n π-system that is intrinsically susceptible to redox events,[8,9] and redox non-innocence that can potentially support unusual reactivity. Chelation of titanium(II) by (dadi)$^{2-}$ was a target, with the expectation that RNI leading to (dadi)$^{4-}$-Ti(IV) could potentially stabilize the system, as the tetraanion has a 4n + 2 π-

^{a}Cornell University, Dept. Chemistry & Chemical Biology, Baker Laboratory, Ithaca, NY, 14853, USA. E-mail: ptw2@cornell.edu

^{b}University of North Texas, Dept. of Chemistry, CASCaM, Denton, TX, 76201, USA. E-mail: t@unt.edu

† Electronic supplementary information (ESI) available. CCDC 1522529–1522531. For ESI and crystallographic data in CIF or other electronic format see DOI: 10.1039/c6sc05610e
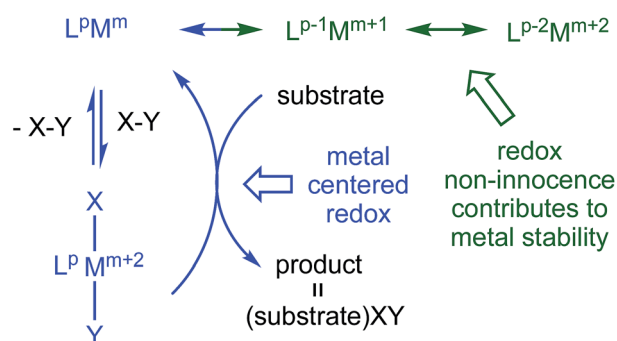
Fig. 1 Conventional oxidative addition (blue), and corresponding 1- and 2-e$^-$ redox non-innocent (RNI) configurations (green) that can electronically buffer the metal center. The ligand, L^p, π-system can be (4n + 2) → 4n or 4n → (4n − 2) depending on its compatibility with M^m.

system. This report describes (dadi)Ti(X/L) species that manifest RNI, including a rare instance in which carbon monoxide does not affect redox activity at the metal, and does not bind, thus permitting its use as a substrate in catalysis.

Results

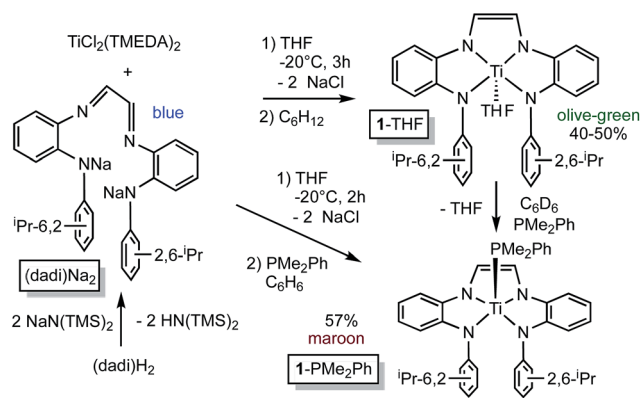### Synthesis of (dadi)TiL$_n$ (n = 1, L = THF, PMe$_2$Ph; n = 2, L = CNMe)

(dadi)Ti(THF). Deprotonation of {−CH═N(1,2-C_6H_4) NH(2,6-$^iPr_2$-C_6H_3)}$_2$, *i.e.*, (dadi)H$_2$,[1] with 2 equiv. NaN(TMS)$_2$ afforded the disodium salt of (dadi)$^{2-}$ in 94% yield according to Scheme 1. The dianion is bright blue in THF solution, and exhibits a dominant absorption band at 770 nm (ε = 22 000 M^{-1} cm^{-1}) that features a ∼1500 cm^{-1} progression plausible for a diimine.

Scheme 1 Synthesis of (dadi)Na$_2$ and (dadi)TiL (L = THF, **1**-THF; PMe$_2$Ph, **1**-PMe$_2$Ph).

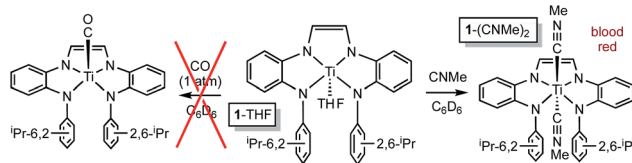**Scheme 2** Methylisocyanide binds, but CO does not.

Treatment of (TMEDA)$_2$TiCl$_2$ (ref. 21) with (dadi)Na$_2$ in THF at -20 °C for 3 h yielded a green solution. After filtration in cyclohexane, (dadi)Ti(THF) (**1**-THF) was isolated in $\sim$40–50% yields as an olive-green powder that contained some residual C$_6$H$_{12}$. The five-coordinate environment of diamagnetic **1**-THF renders the isopropyl groups inequivalent in its ^{1}H NMR spectrum due to hindered rotation of the aryl, and they are observed as doublets in a $\sim$12 : 6 : 6 ratio along with THF resonances.

For related complexes (dadi)M (M = Fe, Mn),[1] the aforementioned, attenuated intraligand (IL) band was split into components at $\sim$720 nm and $\sim$940 nm ($\varepsilon \sim$ 5–12 000 M^{-1} cm^{-1}) in the UV-vis spectrum. Blue shifted, low intensity features at 495 ($\varepsilon \sim$ 900 M^{-1} cm^{-1}) and 590 nm ($\varepsilon \sim$ 700 M^{-1} cm^{-1}) in **1**-THF are remnants of these IL bands according to TDDFT calculations, and are accompanied by a major absorption at 345 nm ($\varepsilon = 32\,000$ M^{-1} cm^{-1}). The spectrum suggested a more covalent electronic environment than in the high spin Fe and Mn species, and calculations support a [(dadi)$^{4-}$](THF)Ti(IV) configuration in which the tetraanionic, tetradentate chelate possesses a 22e$^-$ (4n + 2) π-system.

Unlike previous systems,[10] the ^{1}H NMR spectroscopic chemical shift of the diimine hydrogens, δ 6.64 in (dadi)Ti(THF) (**1**-THF), does not distinguish between redox states of (dadi)^n. Calculations of pseudo-square planar (dadi)Ti (**1**) suggest that it would be best considered [(dadi)$^{3-\downarrow}$]Ti(III)$^\uparrow$, a d^1 titanium antiferromagnetically coupled to (dadi)$^{3-}$, but adduct formation causes an electronic reorganization to the [(dadi)$^{4-}$](L)Ti(IV) configuration.

(dadi)Ti(PMe$_2$Ph). Crystals amenable to an X-ray structural determination of the THF-adduct were elusive, thus a PMe$_2$Ph derivative, (dadi)TiPMe$_2$Ph (**1**-PMe$_2$Ph) was prepared *in situ* by adding the phosphine subsequent to metalation, as shown in Scheme 1. The maroon phosphine adduct, which also manifests a normal diimine ^{1}H NMR spectroscopic shift at δ 6.73, can also be made in a stepwise fashion *via* substitution of THF from **1**-THF.

(dadi)Ti(CNMe)$_2$. In contrast, exposure of **1**-THF to carbon monoxide (1 atm) resulted in no displacement of THF by CO (Scheme 2). d^2 titanium center would likely provide a favorable backbonding to a carbonyl ligand, whereas a more electrophilic

[(dadi)$^{4-}$]Ti(IV) configuration would favor σ-donors. It is noteworthy that MeNC binds to the titanium center to generate blood red (dadi)Ti(CNMe)$_2$ (**1**-(CNMe)$_2$). As in the mono-adducts, **1**-(CNMe)$_2$ also exhibits a normal diimine hydrogen chemical shift (δ 6.16) in its ^{1}H NMR spectrum, and a broad ν(NC) at 2199 cm^{-1} in its IR spectrum. The latter is well above the stretching frequency of free MeNC (2164 cm^{-1}), consistent with a lack of π-backbonding, and indicative of a (dadi)$^{4-}$ formulation.

Structural studies of (dadi)TiL$_n$ (L = PMe$_2$Ph, L$_2$ = (CNMe)$_2$)

(dadi)Ti(PMe$_2$Ph). The X-ray structure determination of (dadi)TiPMe$_2$Ph (**1**-PMe$_2$Ph) supports the [(dadi)$^{4-}$](PhMe$_2$Ph)Ti(IV) electronic configuration. Fig. 2 illustrates a molecular view of **1**-PMe$_2$Ph, revealing a pseudo-square pyramidal structure that is distorted from phosphine–isopropyl interactions. The PMe$_2$Ph is tilted toward the diimine ($\angle$P–Ti–N$_{im}$ = 85.22(2)° (ave)) and the orientation of its phenyl group causes the P–Ti–N1 angle (114.64(6)°) to be greater than the other amide ($\angle$P–Ti–N4 = 123.37(5)°).

The crucial d(CN$_{im}$) of 1.379(3) and 1.381(3) Å are significantly longer than the expected 1.30 Å for a neutral imine,[18,19,22] and the d(C$_{im}$C$_{im}$) is also anomalous at 1.338(3) Å, a value substantially shorter than a C(sp^2)–C(sp^2) distance of 1.43 Å.[22]
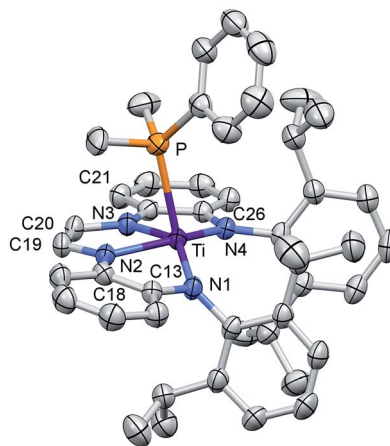
Fig. 2 Molecular view of (dadi)TiPMe$_2$Ph (**1**-PMe$_2$Ph). Interatomic distances (Å) and angles (°): Ti–P, 2.6049(7); Ti–N1, 2.0029(18); Ti–N2, 2.0194(18); Ti–N3, 2.0332(18); Ti–N4, 2.0088(18); N1–C13, 1.411(3); C13–C18, 1.413(3); N2–C18, 1.396(3); N2–C19, 1.379(3); C19–C20, 1.338(3); N3–C20, 1.381(3); N3–C21, 1.396(3); C21–C26, 1.408(3); N4–C26, 1.406(3); P–Ti–N1, 114.64(6); P–Ti–N2, 85.21(5); P–Ti–N3, 85.23(5); P–Ti–N4, 102.35(5); N1–Ti–N2, 78.10(7); N1–Ti–N3, 143.60(7); N1–Ti–N4, 123.37(7); N2–Ti–N3, 73.38(7); N2–Ti–N4, 148.83(7); N3–Ti–N4, 77.14(7).

Titanium–nitrogen distances to the "imines" are also short, at 2.0194(18) and 2.0332(18) Å, values that reflect greater covalency in the interaction of the tetraamide chelate to the Ti(IV) center. For comparison, the "diimine" Ti–N distances are nearly the same as the titanium arylamide–nitrogen bond lengths of 2.0029(18) and 2.0088(18) Å.

(dadi)Ti(CNMe)$_2$. Fig. 3 illustrates the (dadi)Ti(CNMe)$_2$ (**1**-(CNMe)$_2$) molecule, and select core distance and angles are given in the caption. Although **1**-(CNMe)$_2$ is six-coordinate, all dadi metric parameters are within 0.015 Å to those corresponding to (dadi)TiPMe$_2$Ph (**1**-PMe$_2$Ph), with d(C19–C20) = 1.350(3) Å, and d(CN$_{im}$) = 1.372(2) (ave),[18,19,22] consistent with a [dadi]$^{4-}$ (CNMe)$_2$ Ti(IV) formulation, as predicted by the its IR spectrum. The d(Ti–N) are within 0.035 Å at 2.050(18) Å (ave), and describe four amide linkages, although slightly longer than in **1**-PMe$_2$Ph (2.016(13) Å (ave)). The dadi bite angles of N$_{am}$-TiN$_{im}$ and N$_{im}$TiN$_{im}$ are 76.94(15)° (ave) and 73.96(6)°, essentially the same as in the phosphine adduct.

Electronic structure of (dadi)Ti(PMe$_2$Ph)

The metric parameters found in X-ray crystal structure of (dadi)TiPMe$_2$Ph (**1**-PMe$_2$Ph) prompted an electronic structure investigation to assess the proposed RNI. Fig. 4 illustrates a truncated molecular orbital diagram featuring three filled orbitals, with a diimine CC–π-bonding orbital as the HOMO. The unfilled orbitals, predominantly 3d in character, are tightly packed, and well separated from the others, partly as a consequence of DFT calculations.[23] Orbitals d$_{xz}$ and d$_{yz}$ possess modest π-character, but are empty, as expected for the (dadi)$^{4-}$ formulation. Overall, the "3d" orbitals are essentially non-bonding, due to the multicomponent mixing intrinsic to low
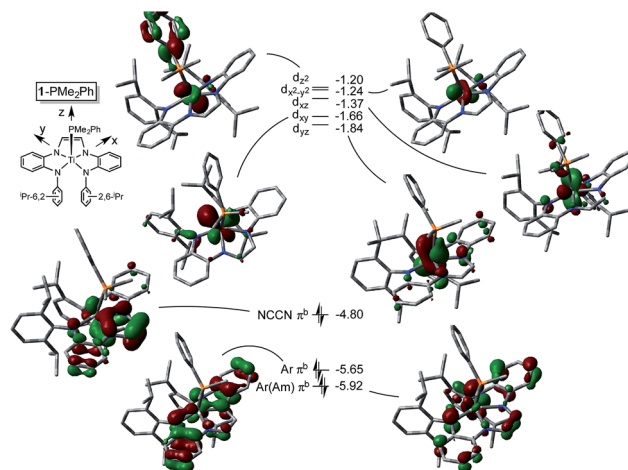

Fig. 4 Truncated MO diagram of (dadi)TiPMe$_2$Ph (**1**-PMe$_2$Ph), showing the unfilled orbitals of the d^0 species, and three filled dadi-based orbitals (energies in eV). Assignments are tentative due to the low symmetry: M06/6-311+G(d) single point calculations for orbitals at the ONIOM(M06/6-311+G(d)) optimized minimum derived from the X-ray structure as an initial guess.

symmetry systems. All filled orbitals shown possess some d-character, so even though dadi is expressed as tetranionic, the metal/dadi admixture reflects the covalence of the system.

Synthesis of (dadi)Ti=X (X = NAd, O)

(dadi)Ti=NAd. Organoazides were explored as a means to prepare imide derivatives,[23–25] with mixed results.[26–28] Use of Me$_3$SiN$_3$ led to a mixture of products, although NMR spectroscopic signals consistent with (dadi)Ti=NSiMe$_3$ were seen, and 2,6-^{i}Pr$_2$C$_6$H$_3$N$_3$ afforded a complex product devoid of symmetry. Treatment of (dadi)Ti(THF) with adamantyl-azide in benzene effervesced immediately, and maroon-red (dadi)Ti=NAd (**2**=NAd) was isolated in 74% yield, as indicated in Scheme 3. ^{1}H NMR spectra revealed an integrated 6 : 12 : 6 ratio of CH(CH$_3$)$_2$ hydrogens, suggestive of a five-coordinate imide complex.

(dadi)Ti=O. Generation of the corresponding oxo complex proved to be equally interesting. Initially, common oxygen atom
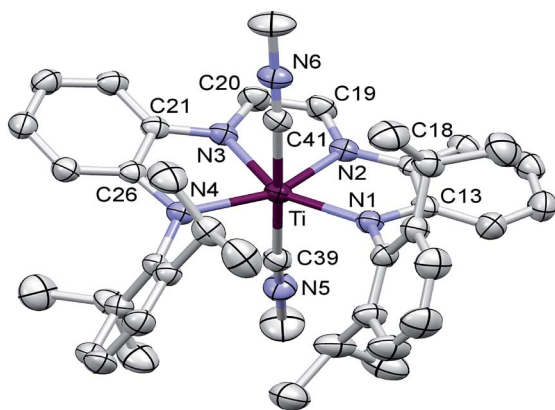

Fig. 3 Molecular view of (dadi)Ti(CNMe)$_2$ (**1**-(CNMe)$_2$). Interatomic distances (Å) and angles (°): Ti–N1, 2.0677(16); Ti–N2, 2.0331(15); Ti–N3, 2.0353(16); Ti–N4, 2.0636(15); Ti–C39, 2.2484(18); Ti–C41, 2.2364(18); N1–C13, 1.396(2); C13–C18, 1.418(3); N2–C18, 1.403(2); N2–C19, 1.373(2); C19–C20, 1.350(3); N3–C20, 1.371(2); N3–C21, 1.401(2); C21–C26, 1.423(2); N4–C26, 1.395(2); C39–N5, 1.141(2); C41–N6, 1.145(2); N1–Ti–N2, 77.04(6); N1–Ti–N3, 149.95(6); N1–Ti–N4, 132.75(6); N2–Ti–N3, 73.96(6); N2–Ti–N4, 150.05(6); N3–Ti–N4, 76.83(6); N1–Ti–C39, 91.41(6); N2–Ti–C39, 84.33(6); N3–Ti–C39, 93.42(6); N4–Ti–C39, 90.98(6); N1–Ti–C41, 91.37(6); N2–Ti–C41, 92.30(6); N3–Ti–C41, 82.13(6); N4–Ti–C41, 90.14(6); C39–Ti–C41, 175.04(7).
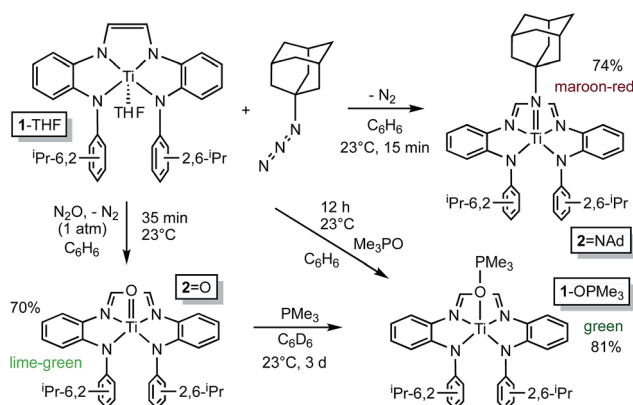
Scheme 3 Imide, (dadi)Ti=NAd (**2**=NAd), and oxo, (dadi)Ti=O (**2**=O), formation from (dadi)Ti(THF) (**1**-THF), AdN$_3$ and N$_2$O, respectively.

transfer (OAT) agents, such as PhIO, Me₃NO, and PyN-O failed, but unexpectedly, nitrous oxide[29–34] proved fruitful. Exposure of (dadi)Ti(THF) (**1**-THF) to N₂O (1 atm) in benzene for ~30 min afforded a lightening of the green solution, and lime green (dadi)TiO (**2**-O) was eventually precipitated from benzene in 70% yield, as Scheme 3 illustrates. Four sets of isopropyl-methyl doublets were observed in the ¹H NMR spectrum in a 6 : 6 : 6 : 6 ratio, and a resonance Raman (λ = 475 nm) spectrum showed an absorption at 1015.4 cm⁻¹ tentatively assigned to the N(TiO).[29] OAT from (dadi)TiO (**2**=O) was tested with a variety of substrates (olefins, CO, etc.), but only transfer to PMe₃, resulting in green (dadi)Ti–OPMe₃ (**1**-OPMe₃), was observed. The latter compound was independently prepared from (dadi)Ti(THF) (**1**-THF) and 1 equiv. of Me₃PO.

Structural study of (dadi)TiO

A molecular view of (dadi)TiO (**2**=O) and accompanying metric parameters are given in Fig. 5. The core O–Ti–N angles average 105.2(4)°, except for ∠O–Ti–N3 = 94.71(5)°, as the oxo tilts slightly toward N3. The diimine bite angle of 71.44(5)°, imine-amide bite angles averaging 75.7(4)°, and the opening N1–Ti–N4 angle of 124.02(5)° describe a slightly distorted square pyramid with basal nitrogens and the apical oxo. The dadi backbone contains d(CN) = 1.299(3) (ave) Å and d(CC) = 1.433(3) Å, consistent with a neutral diimine fragment of a (dadi)²⁻ ligand.[18,19,22] The titanium–nitrogen bond lengths to the diimine are 2.1603(13) and 2.1938(12) Å, substantially longer than the electrostatically contracted d(TiN) of the (dadi)⁴⁻ ligand of (dadi)TiPMe₂Ph (**1**-PMe₂Ph) and (dadi)Ti(CNMe)₂ (**1**-(CNMe)₂). The d(TiO) of 1.6361(11) Å is typical for the numerous Ti(ɪᴠ) oxo species that have been characterized (1.63(1) Å ave for 15 5-coord examples), and the remaining amide distances are typical (2.059(7) (ave) Å).
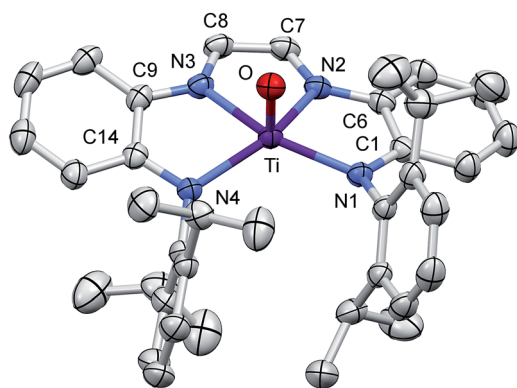
Electronic structure of (dadi)TiO

The electronic structures of (dadi)TiO (**2**=O) and (dadi)Ti=NAd (**2**=NAd) were investigated as examples of species in which the chelate was dianionic. The calculation of **2**=O is featured herein, since the experimental structure is available for comparison. As Fig. 6 illustrates, the TiO π-bonding orbitals are buried below a group of occupied dadi-π-orbitals, including the HOMO, which has significant Npπ-character, but no metal constituent. These contain components of NCCN bonding, but there are no discrete "diimide" orbitals, although a pair of unoccupied orbitals, including the LUMO, are clearly NCCN π* in character. The diagram is consistent with the claim of a highly delocalized (dadi)²⁻ ligand attached to a titanyl fragment, whose π-bonds are clearly rendered at −8.23 and −8.59 eV.

The distortion in (dadi)TiO (**2**=O), reproduced by calculation, appears to be steric in origin, as removal of the 2,6-ⁱPr₂-C₆H₃ groups and re-optimization of the geometry leads to a more symmetric species. Note the similarities in the diagrams of (dadi)TiPMe₂Ph (**1**-PMe₂Ph) and **2**=O, which both show significant gaps between dadi π-system orbitals, an NCCN π*-orbital, and ligand antibonding and metal orbitals. While both diagrams depict Ti(ɪᴠ), the middle NCCN π*-orbital is empty for **2**=O, i.e., (dadi)²⁻, while it is filled for **1**-PMe₂Ph, i.e., (dadi)⁴⁻, thereby revealing disparate redox states for each.

Catalytic carbonylation of adamantyl azide

The RNI of (dadi)ⁿ is implicit in the failure of CO to compete with THF in binding to titanium,[11–13] rendering it capable of catalyzing carbonylation reactions. Scheme 4 illustrates

Fig. 5 Molecular view of (dadi)TiO (**2**=O). Interatomic distances (Å) and angles (°): Ti–O, 1.6361(11); Ti–N1, 2.0538(13); Ti–N2, 2.1938(12); Ti–N3, 2.1603(13); Ti–N4, 2.0640(12); N1–C1, 1.3770(19); C1–C6, 1.419(2); N2–C6, 1.395(2); N2–C7, 1.301(2); C7–C8, 1.433(2); N3–C8, 1.297(2); N3–C9, 1.388(2); C9–C14, 1.418(2); N4–C14, 1.3750(19); O–Ti–N1, 105.18(5); O–Ti–N2, 104.88(5); O–Ti–N3, 94.71(5); O–Ti–N4, 105.66(5); N1–Ti–N2, 75.40(5); N1–Ti–N3, 144.73(5); N1–Ti–N4, 124.02(5); N2–Ti–N3, 71.44(5); N2–Ti–N4, 136.56(5); N3–Ti–N4, 75.94(5).
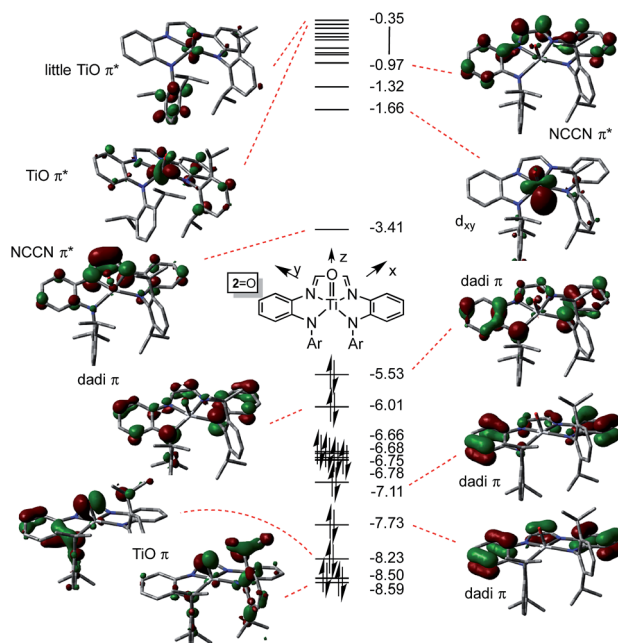

Fig. 6 Truncated molecular orbital diagram of (dadi)TiO (**2**=O); orbitals not plotted are either diffuse virtual orbitals or pertain to 2,6-ⁱPr₂C₆H₃. Energies are in eV.

a plausible mechanism for the carbonylation of the nitrene derived from adamantyl azide (>20 turnovers) as catalyzed by (dadi)Ti=NAd (**2**=NAd). Insertion of the carbonyl into the titanium–imide bond, perhaps *via* an initial *cis*-bonding event, affects formation of an isocyanate adduct, and subsequent substitution by AdN_3, dissociative, associative, or interchange, generates an azide adduct that releases N_2 to restart the cycle.

Imide (dadi)Ti=NAd (**2**=NAd) is the only metal-containing species observed when the catalysis is monitored by ^1H NMR spectroscopy, and its concentration diminishes during the course of catalysis. The catalysis was modeled by a two-step process in which the imide is clipped from **2**=NAd by CO, and renewed by the reaction of (dadi)Ti (**1**) with AdN_3, as shown in Scheme 5. A degradation path was added to account for loss of catalyst over time. Initial kinetics experiments confirmed an order in [CO], and while the concentration of CO in solution was only ~3.5 times that of **2**=NAd, the reaction was slow enough such that CO (~60 fold excess) was replenished from the gas phase. As a consequence CO was a pseudo first-order reagent, and the phenomenological rate ($-d[AdN_3]/dt = k_{obs}$; $k_{obs} = k_{CO}[\mathbf{2}=NAd][CO]$) was zero-order since the catalyst concentration also does not change, aside from the degradation. Factoring out [CO] and [**2**=NAd] afforded a second-order rate constant for carbonylation as $3.13(24) \times 10^{-3}$ M^{-1} s^{-1} ($\Delta G^{\ddagger}$ (55 °C) = 23.0(1) kcal mol^{-1}), as listed in Table 1.

A stoichiometric study supported carbonylation as the rate-determining elementary step in the catalysis. Treatment of **2**=NAd with an excess of CO (pseudo first-order, 3.1–3.6 atm) in C_6D_6 (with THF present) at 25–75 °C afforded AdNCO, and (dadi)Ti(THF) (**1**-THF), presumably resulting from trapping of (dadi)Ti (**1**). A first-order dependence on [CO] was found ($-d[\mathbf{2}=NAd]/dt = k_{CO}[\mathbf{2}=NAd][CO]$), and an Eyring analysis of the second order rate constants listed in Table 1 yielded a $\Delta H^{\ddagger}$ of 9.6(9) kcal mol^{-1}, and a $\Delta S^{\ddagger}$ of −39.9(28) eu. The calculated $\Delta G^{\ddagger}$ at 55 °C is 22.6(9) kcal mol^{-1}, a value consistent with that obtained during catalysis, supporting the claim of carbonylation as the rate-determining step. The modest enthalpy of activation
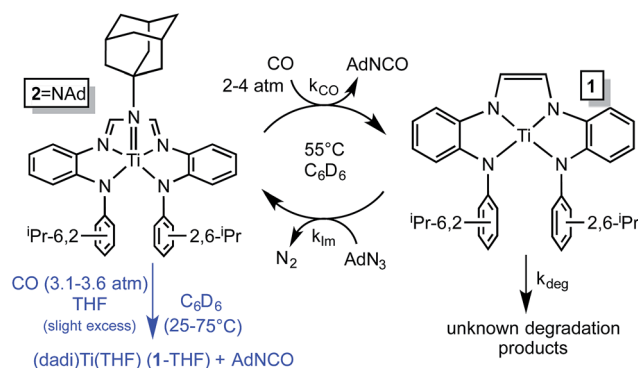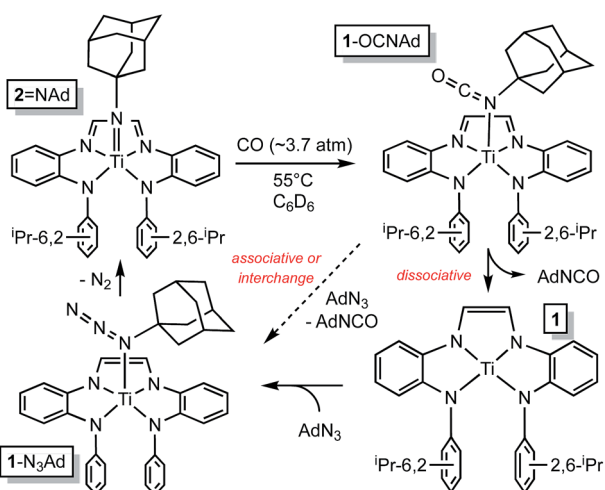

Scheme 5 Kinetic model for AdN_3 carbonylation catalysis by **2**=NAd (black) and stoichiometric study of imide carbonylation (blue).

Table 1 Kinetics of **2**=NAd carbonylation, stoichiometric and catalytic, in C_6D_6

2=NAd (M)	CO^a (M)	T (°C)	$k_{CO} \times 10^3$ (M^{-1} s^{-1})	$\Delta G^{\ddagger}$ (kcal mol^{-1})
0.047^b	0.023	25.0(5)	1.25(6)	21.4(1)
0.048^b	0.025	35.0(5)	1.83(8)	21.9(1)
0.047^b	0.026	45.0(5)	3.58(15)	22.2(1)
0.047^{b,c}	0.028	55.0(5)	5.44(42)	22.7(1)
0.047^b	0.030	65.0(5)	7.95(86)	23.1(1)
0.047^b	0.033	75.0(5)	14.0(11)	23.4(1)
0.047^c	0.0105	55.0(5)	4.62(69)	22.8(1)
0.046^c	0.023	55.0(5)	4.20(45)	22.8(1)
0.0063^d	0.022	55.0(5)	3.13(24)	23.0(1)

^{a} Calculated from Henry's law and corrected for temperature dependence. ^{b} Rate constants obtained from an average of three trials; from a weighted Eyring plot: $\Delta H^{\ddagger} = 9.6(9)$ kcal mol^{-1}, $\Delta S^{\ddagger} = -39.9(28)$ eu, $\Delta G^{\ddagger}$ (55 °C) = 22.6(9) kcal mol^{-1}. An unweighted Eyring plot gives: $\Delta H^{\ddagger} = 9.3(4)$ kcal mol^{-1}, $\Delta S^{\ddagger} = -40.7(13)$ eu, $\Delta G^{\ddagger}$ (55 °C) = 22.6(6) kcal mol^{-1}. ^{c} To determine order in CO; $k_{obs} = 4.85(55) \times 10^{-5}$ s^{-1} at [CO] = 0.0105 M; $k_{obs} = 9.67(95) \times 10^{-5}$ s^{-1} at [CO] = 0.023 M; $k_{obs} = 1.52(8) \times 10^{-4}$ s^{-1} at [CO] = 0.028 M. ^{d} Catalytic rate obtained from fitting disappearance of [AdN_3] and [**2**=NAd] according to Scheme 5 (3 trials): p(CO) = 2.58 atm, total mol CO = 1.82×10^{-4}, [AdN_3] = 0.123 M, $k_{deg} = 3.2(3) \times 10^{-5}$ Ms^{-1}. See ESI for details.
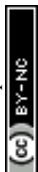
thus reflects the balance between N=C bond-formation and Ti=N bond-breaking in the transition state, while the large negative entropy of activation value is consistent with a 2nd-order process.

Calculated free energy profile of AdN_3 carbonylation

Fig. 7 illustrates the calculated free energy profile for the catalytic carbonylation of AdN_3 to AdNCO + N_2, a reaction that is exergonic by −72.8 kcal mol^{-1}. Formation of the C=N bond in AdNCO is −72.3 kcal mol^{-1} enthalpically more favorable than the corresponding azide N=N bond in terms of free energy, and constitutes the driving force for catalysis.

The calculated $\Delta G^{\ddagger}$ (298.15 K) for carbonylation of the imide, (dadi)Ti=NAd (**2**=NAd) is 20.9 kcal mol^{-1}, in decent agreement with experiment (21.5 kcal mol^{-1} at 25 °C). The slight

Scheme 4 Plausible mechanisms for the catalyzed conversion of AdN_3 + CO → AdNCO + N_2 by the imide, (dadi)Ti=NAd (**2**=NAd).
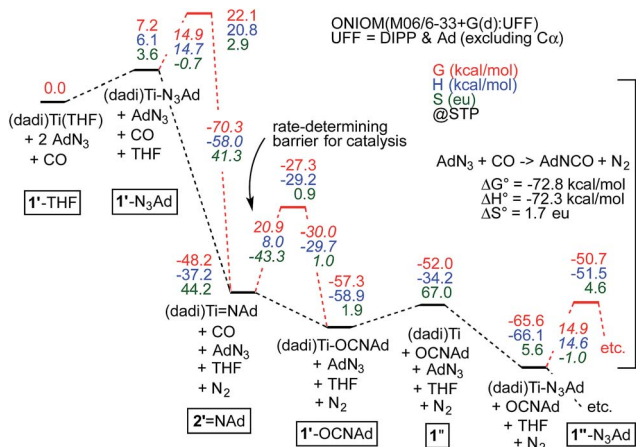
Fig. 7 Calculations of Scheme 4, with transition states (primes indicate calculated states; activation energies italicized) pertaining to N_2 loss from bound azide, (dadi)Ti(N_3Ad) (**1**-N_3Ad) and carbonylation of (dadi)Ti=NAd (**2**=NAd). Association/dissociation transition states are not included. Small inconsistencies are due to round-off errors. Calculated **1**′-L and **1**″-L compounds have (dadi)$^{4-}$ configurations, **2**′=NAd has a (dadi)$^{2-}$ structure, and **1**″ is computed as [(dadi)$^{3-\downarrow}$]Ti(III)$^{\uparrow}$.

discrepancy is spread between $\Delta H^{\ddagger}$ (calc'd 8.0 kcal mol^{-1}) and $\Delta S^{\ddagger}$ (calc'd -43.3 eu). The latter is similar to the calculated $\Delta S^{\ddagger} = -42.3$ eu for the microscopic reverse of N_2 extrusion from (dadi)Ti(N_3Ad) (**1**-N_3Ad). Formation of (dadi)Ti (**1**) + AdNCO from **2**=NAd and CO is only favorable by $\Delta G^{\circ} = -3.8$ kcal mol^{-1}, and enthalpically unfavorable by $\Delta H^{\circ} = 3.0$ kcal mol^{-1}, hence carbonylation has modest thermodynamic impetus. With the Bond Dissociation Enthalpy (BDE(calc)) of the AdN=CO bond at 81 kcal mol^{-1}, the titanium–imide bond BDE(calc) is $\sim$84 kcal mol^{-1}.[35] Both adducts, **1**-N_3Ad and **1**-OCNAd, are calculated to be most stable as κ^1-NAd-bound species.

Dinitrogen loss from **1**-N_3Ad possesses the next highest transition state, at $\Delta G^{\ddagger} = 14.9$ kcal mol^{-1}. The binding of AdN$_3$ to (dadi)Ti is favorable by only -13.6 kcal mol^{-1}, but the subsequent loss of N_2 to form **2**=NAd is substantial, at -55.4 kcal mol^{-1}, hence there is substantial thermodynamic influence on the dinitrogen loss step. Associative or interchange transition states for AdN$_3$ displacement of isocyanate from **1**-OCNAd could not be found. Since dissociation of product OCNAd from **1**-OCNAd is calculated to be only $\Delta G^{\circ} = 5.3$ kcal mol^{-1}, it is unlikely that steps subsequent to carbonylation, and preceding loss of N_2 from **1**-N_3Ad are particularly consequential.

Discussion

Transfers of X (NAd, O) from (dadi)Ti=X

In the successful transfer of the imido functionality of (dadi)Ti=NAd (**2**-Ad) to CO, affording AdNCO, the redox non-innocence of the dadi ligand was critical. Stabilization of presumed transient (dadi)Ti (**1**) as [(dadi)$^{3-\downarrow}$]Ti(III)$^{\uparrow}$, (dadi)TiL (**1**-L) via (dadi)$^{4-}$, and **2**-Ad through (dadi)$^{2-}$ permits the titanium to exist in favorable, higher oxidation states while catalyzing the carbonylation, providing a textbook example of the RNI in Fig. 1.

The dadi ligand is more oxidizing to the titanium center than one or two bound CO ligands, possessing the 22 πe$^-$ ($4n + 2$)

configuration in (dadi)TiL (**1**-L), but less oxidizing than a nitrene (*i.e.*, NAd), where it resides in its 20 πe$^-$ ($4n$) form. The MO diagrams for (dadi)TiPMe$_2$Ph (**1**-PMe$_2$Ph) and (dadi)Ti=O (**2**=O), if taken as analogues for a potential carbonyl species, and (dadi)Ti=NAd (**2**-Ad), respectively, support this key electronic rationale. Concerning Fig. 4 (**1**-PMe$_2$Ph), any backbonding interaction with one of the dπ-orbitals would have to lower it below -4.80 eV in order to depopulate the NCCN π-orbital and render the dadi dianionic. Apparently CO, a potent π-acid toward titanium, is incapable of inducing the necessary change. Note that in Fig. 6 (**2**=O), the related NCCN π-orbital at -3.41 eV is the LUMO in the system, having been depopulated in favor of the oxo π-bonding orbitals of low energy.

The catalytic carbonylation in Scheme 4 produces AdNCO, but fortunately OAT to afford (dadi)TiO (**2**=O) and CNAd is calculated to be only slightly favorable ($\Delta G^{\circ} = -1.1$ kcal mol^{-1}).[36,37] The released CNAd is also favored to scavenge any (dadi)Ti (**1**) and provide (dadi)Ti(CNAd) with $\Delta G^{\circ}_{\text{calcd}} = -22.1$ kcal mol^{-1}. It is likely that the barrier for OAT from AdNCO is sluggish compared to dinitrogen loss from (dadi)Ti(N_3Ad) (**1**-N_3Ad) to form (dadi)Ti=NAd (**2**-Ad), because the latter is exergonic by $\Delta G^{\circ}_{\text{calcd}} = -69.0$ kcal mol^{-1}. Since all adduct formations are expected to be rapid and reversible, OAT is likely not competitive. Note that no IR spectral evidence of isocyanide formation is observed in catalytic runs, even at the end of catalysis.

Attack by PMe$_3$ on (dadi)TiO (**2**=O) to form (dadi)TiOPMe$_3$ (**1**-OPMe$_3$) is calculated to be favorable by $\Delta G^{\circ} = -22.5$ kcal mol^{-1}, but is relatively slow (>24 h, 23 °C), presumably due to known orbital symmetry constraints on OAT.[38] The phosphine oxide adduct is more favorable than (dadi)Ti(THF) (**1**-THF) by $\Delta G^{\circ}_{\text{calcd}} = -17.2$ kcal mol^{-1}.

While the ligand redox states are consequential to nitrene transfer, certain atom and group transfers are not so readily explained. For example, the deoxygenation of (dadi)TiO (**2**=O) by CO with 1 equiv. THF present to form (dadi)Ti(THF) (**1**-THF) and CO$_2$ is calculated to be exergonic by $\Delta G^{\circ} = -19.2$ kcal mol^{-1} ($\Delta H^{\circ} = -34.6$ kcal mol^{-1}, $\Delta S^{\circ} = -51.6$ eu).[36,37] Decomposition is observed, perhaps indicative of additional reactivity from liberated CO$_2$; further study is warranted. In addition, attempts to generate other (dadi)Ti=NR (**2**=NR) species[23–25] led to unanticipated reactivity, hence the adamantyl group protects the imide in (dadi)Ti=NAd (**2**-Ad) such that group transfer can be realized.

Attempts to catalyze carbodiimide formation akin to Heyduk's zirconium system[12] failed, as treatment of (dadi)Ti=NAd (**2**-Ad) with CNMe afforded (dadi)Ti(CNMe)$_2$ (**1**-(CNMe)$_2$) and only a trace amount of MeNCNAd. Apparently the strong sigma-donation of CNMe, in contrast to the weak donor CO, imparts too much stability to the diisocyanide, as exposure of **1**-(CNMe)$_2$ to AdN$_3$ was also ineffective.

Transition state of imide carbonylation

The transition state (TS) for imide carbonylation of (dadi)Ti=NAd (**2**=NAd) was found via DFT calculations, and views of the TS and its accompanying metrics are illustrated in Fig. 8. The CO attacks the titanium at an angle consistent with its lone pair
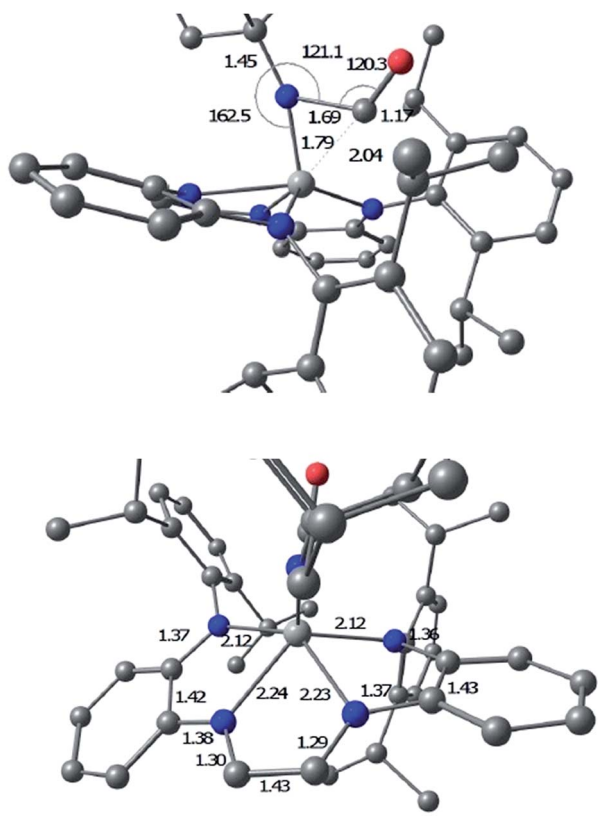
Fig. 8 Views of the computed transition state for carbonyl addition to the imide of (dadi)Ti=NAd (**2**=NAd): (a) metrics (distances (Å), angles (°)) of the imide-carbonyl fragment; (b) distances of the core and dadi ligand.

interacting with d$_{xz/yz}$, while the imide connection is made via an Npπ → COπ* interaction. Related investigations of early metal nitride carbonylations show initial CO binding to be important,[39] and the d(Ti–C) of 1.79 Å shows an interaction with the titanium.

The TS appears early in the reaction coordinate, as the d(TiN) of 1.79 Å is only 0.11 Å longer than the calculated d(TiN) in **2**=NAd, the TiNC(Ad) angle is still large (162.5°), and the d(NC) is long at 1.69 Å. The accompanying NCO angle is 120.3°, significantly bent from the 175° in the calculated κ^1-N-OCNAd adduct that is the initial product of carbonylation, but there is considerable lengthening of the d(CO) to 1.17 Å. The calculated metrics pertaining to the TS (dadi)Ti core still conform to (dadi)$^{2-}$, as the 2.12 and 2.14 Å Ti–N$_{am}$ distances are significantly shorter than the Ti–N$_{im}$ bond lengths of 2.23 and 2.24 Å. In a late TS, the core geometry would be expected to more closely correspond to (dadi)$^{4-}$, which is calculated to have similar amide and "imine" d(TiN).

Conclusions

Structural and computational investigations show that dadi^m is capable of binding as a tetraanion in [dadi^{4-}]Ti(IV)L$_x$ (**1**-L$_x$; L$_x$ = THF, PMe$_2$Ph, (CNMe)$_2$) and as a dianion in [dadi^{2-}]Ti(IV)X (**2**=X; X = O, NAd). The redox non-innocence of dadi^m is crucial in making CO binding to (dadi)Ti essentially devoid of π-backbonding, and uncompetitive with THF adduct

formation by $\Delta G°$(calc'd) = 7.7 kcal mol^{-1}. In contrast, formation of oxo or adamantyl-imido multiple bonds is competitive with dadi reduction, ultimately permitting the successful catalytic carbonylation of AdN$_3$ in which the redox changes occur at dadi rather than titanium.

Carbonylation catalysis with titanium is quite unusual, with Buchwald's enone synthesis as the primary example,[40] and catalytic nitrene transfer from titanium is limited to Tonks' recent pyrrole synthesis.[41] While the former is unlikely to involve formal RNI, the capability of Cp to covalently distribute charge is remarkable;[42] a bound pyrrole product in the latter system could act in a redox non-innocent fashion.

Experimental section

Full experimental details are given in the ESI,† including kinetics and computational procedures in addition to syntheses. Brief descriptions of the syntheses, kinetic measurements, and computations are given in the schemes, and figure and table captions. Elemental analyses on all (dadi)Ti-based compounds failed normal standards, despite multiple attempts on crystalline samples, and utilization of several companies. As a consequence, full spectral characterizations, including all pertinent NMR spectra, are provided in the ESI.†

Crystal data for **1**-PMe$_2$Ph: C$_{46}$H$_{55}$N$_4$PTi, M = 742.81, monoclinic, $P2_1/c$, a = 18.3497(6), b = 10.3436(3), c = 25.5974(8) Å, β = 108.022(2)°, V = 4620.1(3) Å^3, T = 223(2) K, λ = 0.71073 Å, Z = 4, R_{int} = 0.0524, 40 189 reflections, 8152 independent, R_1(all data) = 0.0672, wR_2 = 0.1340, GOF = 1.048, CCDC-1522529.

Crystal data for **1**-(CNMe)$_2$: C$_{47}$H$_{62}$N$_6$Ti, M = 758.92, triclinic, P-1, a = 10.2323(6), b = 13.2844(7), c = 16.9919(9) Å, α = 100.164(3)° β = 104.521(2)° γ = 95.151(2)°, V = 2179.0(2) Å^3, T = 223(2) K, λ = 0.71073 Å, Z = 2, R_{int} = 0.0344, 29 680 reflections, 8887 independent, R_1(all data) = 0.0639, wR_2 = 0.1178, GOF = 1.026, CCDC-1252531.

Crystal data for **2**=O: C$_{49}$H$_{62}$N$_4$OTi, M = 770.92, triclinic, P-1, a = 13.1179(8), b = 13.2082(8), c = 13.7748(8) Å, α = 105.738(3)° β = 99.727(3)° γ = 98.022(3)°, V = 2220.5(2) Å^3, T = 223(2) K, λ = 0.71073 Å, Z = 2, R_{int} = 0.0313, 40 966 reflections, 9425 independent, R_1(all data) = 0.0532, wR_2 = 0.1215, GOF = 1.041, CCDC-1522530.

Acknowledgements

Notes and references

1 S. P. Heins, W. D. Morris, P. T. Wolczanski and E. B. Lobkovsky, *Angew. Chem., Int. Ed.*, 2015, **54**, 14407–14411.

2 L. A. Berben, B. de Bruin and A. G. Heyduk, *Chem. Commun.*, 2015, **51**, 1553–1554.

3 (a) W. I. Dzik, J. I. van der Vlugt, J. N. H. Reek and B. de Bruin, *Angew. Chem., Int. Ed.*, 2011, **50**, 3356–3358; (b) V. Lyaskovskyy and B. de Bruin, *ACS Catal.*, 2012, **2**, 270–279.

4 R. F. Munhá, R. A. Zarkesh and A. F. Heyduk, *Dalton Trans.*, 2103, **42**, 3751–3766.

5 P. J. Chirik, *Acc. Chem. Res.*, 2015, **48**, 1687–1695.

6 K. G. Caulton, *Eur. J. Inorg. Chem.*, 2012, 435–443.

7 K. Ray, T. Petrenko, K. Wieghardt and F. Neese, *Dalton Trans.*, 2007, 1552–1566.

8 V. A. Williams, P. T. Wolczanski, J. Sutter, K. Meyer, E. B. Lobkovsky and T. R. Cundari, *Inorg. Chem.*, 2014, **53**, 4459–4474.

9 W. D. Morris, P. T. Wolczanski, J. Sutter, K. Meyer, T. R. Cundari and E. B. Lobkovsky, *Inorg. Chem.*, 2014, **53**, 7467–7484.

10 B. A. Frazier, P. T. Wolczanski, I. Keresztes, S. DeBeer, E. B. Lobkovsky, A. W. Pierpont and T. R. Cundari, *Inorg. Chem.*, 2012, **51**, 8177–8186.

11 A. F. Heyduk, R. A. Zarkesh and A. I. Nguyen, *Inorg. Chem.*, 2011, **50**, 9849–9863.

12 (a) A. I. Nguyen, R. A. Zarkesh, D. C. Lacy, M. K. Thorson and A. F. Heyduk, *Chem. Sci.*, 2011, **2**, 166–169; (b) K. J. Blackmore, N. Lal, J. W. Ziller and A. F. Heyduk, *J. Am. Chem. Soc.*, 2008, **130**, 2728–2729; (c) R. A. Zarkesh, J. W. Ziller and A. F. Heyduk, *Angew. Chem., Int. Ed.*, 2008, **47**, 4715–4718.

13 (a) K. J. Blackmore, J. W. Ziller and A. F. Heyduk, *Inorg. Chem.*, 2005, **44**, 5559–5561; (b) M. R. Haneline and A. F. Heyduk, *J. Am. Chem. Soc.*, 2006, **128**, 8410–8411; (c) N. A. Ketterer, H. Fan, K. J. Blackmore, X. Yang, J. W. Ziller, M.-H. Baik and A. F. Heyduk, *J. Am. Chem. Soc.*, 2008, **130**, 4364–4374; (d) A. F. Heyduk, R. A. Zarkesh and A. I. Nguyen, *Inorg. Chem.*, 2011, **50**, 9849–9863; (e) R. F. Munha, R. A. Zarkesh and A. F. Heyduk, *Inorg. Chem.*, 2013, **52**, 11244–11255; (f) S. Hananouchi, B. T. Krull, J. W. Ziller, F. Furche and A. F. Heyduk, *Dalton Trans.*, 2014, **43**, 17991–18000.

14 (a) J. M. Hoyt, K. T. Sylvester, S. P. Semproni and P. J. Chirik, *J. Am. Chem. Soc.*, 2013, **135**, 4862–4877; (b) K. T. Sylvester and P. J. Chirik, *J. Am. Chem. Soc.*, 2009, **131**, 8772–8773; (c) M. W. Bouwkamp, A. C. Bowman, E. Lobkovsky and P. J. Chirik, *J. Am. Chem. Soc.*, 2006, **128**, 13340–13341; (d) S. K. Russell, E. Lobkovsky and P. J. Chirik, *J. Am. Chem. Soc.*, 2011, **133**, 8858–8861; (e) J. M. Darmon, S. C. Stieber, K. L. Sylvester, I. Fernández, E. Lobkovsky, S. P. Semproni, E. Bill, K. Wieghardt, S. DeBeer and P. J. Chirik, *J. Am. Chem. Soc.*, 2012, **134**, 17125–17137.

15 S. S. Karpiniec, D. S. McGuiness, G. J. P. Britovsek and J. Patel, *Organometallics*, 2012, **31**, 3439–3442.

16 R. Sikari, S. Sinha, U. Jash, S. Das, P. Brandão, B. de Bruin and N. D. Paul, *Inorg. Chem.*, 2016, **55**, 6114–6123.

17 (a) A. L. Smith, K. I. Hardcastle and J. D. Soper, *J. Am. Chem. Soc.*, 2010, **132**, 14358–14360; (b) C. A. Lippert, S. A. Arnstein, C. D. Sherrill and J. D. Soper, *J. Am. Chem. Soc.*, 2010, **132**, 3879–3892; (c) C. J. Rolle III, K. I. Hardcastle and J. D. Soper, *Inorg. Chem.*, 2008, **47**, 1892–1894.

18 C. C. Lu, E. Bill, T. Weyhermüller, E. Bothe and K. Wieghardt, *J. Am. Chem. Soc.*, 2008, **130**, 3181–3197.

19 V. A. Williams, E. B. Hulley, P. T. Wolczanski, K. M. Lancaster and E. B. Lobkovsky, *Chem. Sci.*, 2013, **4**, 3636–3648.

20 (a) T. Marshall-Roth and S. N. Brown, *Dalton Trans.*, 2015, 677–685; (b) L. G. Ranis, K. Werellapatha, N. J. Pietrini, B. A. Bunker and S. N. Brown, *Inorg. Chem.*, 2014, **53**, 10203–10206; (c) A. H. Randolph, N. J. Seewald, R. Karl and S. N. Brown, *Inorg. Chem.*, 2013, **52**, 12587–12598.

21 J. J. H. Edema, R. Duchateau, S. Gambarotta, R. Hynes and E. Gabe, *Inorg. Chem.*, 1991, **30**, 154–156.

22 F. H. Allen, O. Kennard, D. G. Watson, L. Brammer, A. G. Orpen and R. Taylor, *J. Chem. Soc., Perkin Trans. 2*, 1987, S1–S19; R. Stowasser and R. Hoffmann, *J. Am. Chem. Soc.*, 1999, **121**, 3414–3420.

23 A. R. Fout, U. J. Kilgore and D. J. Mindiola, *Chem.–Eur. J.*, 2007, **13**, 9428–9440.

24 C. Lorber, R. Choukroun and L. Vendier, *Eur. J. Inorg. Chem.*, 2006, 4503–4518.

25 (a) N. Hazari and P. Mountford, *Acc. Chem. Res.*, 2005, **38**, 839–849; (b) L. Gade and P. Mountford, *Coord. Chem. Rev.*, 2001, **216–217**, 65–97; (c) P. Mountford, *Chem. Commun.*, 1997, 2127–2134.

26 S. D. Gray, J. L. Thorman, L. M. Berreau and L. K. Woo, *Inorg. Chem.*, 1997, **36**, 278–283.

27 S. M. Mullins, A. P. Duncan, R. G. Bergman and J. Arnold, *Inorg. Chem.*, 2001, **40**, 6952–6963.

28 (a) T. E. Hanna, E. Lobkovsky and P. J. Chirik, *Eur. J. Inorg. Chem.*, 2007, 2677–2685; (b) T. E. Hanna, I. Keresztes, E. Lobkovsky, W. H. Bernskoetter and P. J. Chirk, *Organometallics*, 2004, **23**, 3448–3458; (c) I. Pappas and P. J. Chirik, *J. Am. Chem. Soc.*, 2016, **138**, 13379–13389.

29 M. R. Smith III, P. T. Matsunaga and R. A. Andersen, *J. Am. Chem. Soc.*, 1993, **115**, 7049–7050.

30 W. B. Tolman, *Angew. Chem., Int. Ed.*, 2010, **49**, 1018–1024.

31 (a) W. A. Howard, T. M. Trnka, M. Waters and G. Parkin, *J. Organomet. Chem.*, 1997, **525**, 95–121; (b) C. C. Cummins, R. R. Schrock and W. M. Davis, *Inorg. Chem.*, 1994, **33**, 1448–1457.

32 J. T. Groves and J. S. Roman, *J. Am. Chem. Soc.*, 1995, **117**, 5594–5595.

33 N. A. Piro, M. F. Lichterman, W. H. Harman and C. J. Chang, *J. Am. Chem. Soc.*, 2011, **133**, 2108–2111.

34 C. E. Laplaza, A. L. Odom, W. M. Davis, C. C. Cummins and J. D. Protasiewicz, *J. Am. Chem. Soc.*, 1995, **117**, 4999–5000.

35 J. L. Bennett and P. T. Wolczanski, *J. Am. Chem. Soc.*, 1997, **119**, 10696–10719.

36 W. Darwish, E. Seikel, R. Käsmarker, K. Harms and J. Sundermeyer, *Dalton Trans.*, 2011, **40**, 1787–1794.

37 (a) A. E. Guiducci, C. L. Boyd, E. Clot and P. Mountford, *Dalton Trans.*, 2009, 5960–5979; (b) A. E. Guiducci, C. L. Boyd and P. Mountford, *Organometallics*, 2006, **25**, 1167–1187.

38 A. S. Veige, L. M. Slaughter, E. B. Lobkovsky, P. T. Wolczanski, N. Matsunaga, S. A. Decker and T. R. Cundari, *Inorg. Chem.*, 2003, **42**, 6204–6224.

39 (*a*) A. F. Cozzolino, J. S. Silvia, N. Lopez and C. C. Cummins, *Dalton Trans.*, 2014, **43**, 4639–4652; (*b*) J. S. Silvia and C. C. Cummins, *J. Am. Chem. Soc.*, 2009, **131**, 446–447.

40 (*a*) N. M. Kablaoui, F. A. Hicks and S. L. Buchwald, *J. Am. Chem. Soc.*, 1997, **119**, 4424–4431; (*b*) F. A. Hicks and S. L. Buchwald, *J. Am. Chem. Soc.*, 1999, **119**, 7026–7033.

41 Z. W. Gilbert, R. J. Hue and I. A. Tonks, *Nat. Chem.*, 2015, **8**, 63–68.

42 P. T. Wolczanski, *Organometallics*, 2017, **36**, 622–631.